ADVANCES IN ATMOSPHERIC SCIENCES, VOL. 40, APRIL 2023, 587–600

• **Original Paper** •

CMIP6 Evaluation and Projection of Precipitation over Northern China: Further Investigation

Xiaoling YANG[1,2,3], Botao ZHOU*[1,2], Ying XU[4], and Zhenyu HAN[4]

[1]*Collaborative Innovation Center on Forecast and Evaluation of Meteorological Disasters/Key Laboratory of Meteorological Disaster*, *Ministry of Education/Joint International Research Laboratory of Climate and Environment Change*, *Nanjing University of Information Science and Technology*, *Nanjing* 210044, *China*

[2]*School of Atmospheric Sciences*, *Nanjing University of Information Science and Technology*, *Nanjing* 210044, *China*

[3]*Jiangxi Vocational and Technical College of Information Application*, *Nanchang* 330043, *China*

[4]*National Climate Center*, *China Meteorological Admnistration*, *Beijing* 100081, *China*

(Received 28 March 2022; revised 10 August 2022; accepted 31 August 2022)

ABSTRACT

Based on 20 models from phase 6 of the Coupled Model Intercomparison Project (CMIP6), this article explored possible reasons for differences in simulation biases and projected changes in precipitation in northern China among the all-model ensemble (AMME), "highest-ranked" model ensemble (BMME), and "lowest-ranked" model ensemble (WMME), from the perspective of atmospheric circulations and moisture budgets. The results show that the BMME and AMME reproduce the East Asian winter circulations better than the WMME. Compared with the AMME and WMME, the BMME reduces the overestimation of evaporation, thereby improving the simulation of winter precipitation. The three ensemble simulated biases for the East Asian summer circulations are generally similar, characterized by a stronger zonal pressure gradient between the mid-latitudes of the North Pacific and East Asia and a northward displacement of the East Asian westerly jet. However, the simulated vertical moisture advection is improved in the BMME, contributing to the slightly higher performance of the BMME than the AMME and WMME on summer precipitation in North and Northeast China. Compared to the AMME and WMME, the BMME projects larger increases in precipitation in northern China during both seasons by the end of the 21st century under the Shared Socioeconomic Pathway 5-8.5 (SSP5-8.5). One of the reasons is that the increase in evaporation projected by the BMME is larger. The projection of a greater dynamic contribution by the BMME also plays a role. In addition, larger changes in the nonlinear components in the BMME projection contribute to a larger increase in winter precipitation in northern China.

Key words: CMIP6, ensemble evaluation and projection, moisture budget, atmospheric circulation

Citation: Yang, X. L., B. T. Zhou, Y. Xu, and Z. Y. Han, 2023: CMIP6 evaluation and projection of precipitation over Northern China: Further investigation. *Adv. Atmos. Sci.*, **40**(4), 587−600, https://doi.org/10.1007/s00376-022-2092-4.

Article Highlights:

- BMME improvement in the EAWM circulations and evaporation reduces the wet bias of winter precipitation in northern China.
- BMME improvement in the vertical moisture advection slightly enhances the simulation of summer precipitation in North and Northeast China.
- The BMME projection of larger changes in evaporation and dynamic contribution favors a larger increase in the seasonal precipitation in northern China.

1. Introduction

The spatiotemporal change of precipitation patterns in the context of global warming is a topic of particular interest and concern for scientists and policymakers since floods and droughts resulting from abnormal variations exert significant socioeconomic impacts. The development of climate models, coordinated by the Coupled Model Intercomparison Project (CMIP), provides a good opportunity for studying the physical mechanisms, predictions, and projections of precipitation change. Based on the CMIP3/CMIP5 simulations, many studies have been performed to evaluate and project precipitation over China. In general, the CMIP3/CMIP5 models

* Corresponding author: Botao ZHOU
Email: zhoubt@nuist.edu.cn

can reasonably simulate the climatological characteristics of precipitation in China, albeit with systematic biases. Meanwhile, large uncertainties exist in the projection due to different results among models (e.g., Xu and Xu, 2012; Chen and Sun, 2013; Huang et al., 2013; Kumar et al., 2014; Zhou et al., 2014; Tian et al., 2015; Sun et al., 2015; Jiang et al., 2016; Hu et al., 2017; Wang et al., 2017; Zhou et al., 2018b; Rao et al., 2019; Lu et al., 2021). Thus, it is essential to investigate the causes and associated physical processes that explain the simulation biases and different projection behaviors among the models to help improve their simulation ability and reduce the projection uncertainty.

Some studies indicated that the limited performance of models on precipitation is due to their poor simulations of large-scale atmospheric circulations (e.g., Zhou and Li, 2002; Huang et al., 2013; Niu et al., 2015). For example, model bias in the simulated intensity and location of the East Asian westerly jet and the western Pacific subtropical high influence the simulation of summer precipitation in eastern China (Huang et al., 2013; Ren et al., 2017; Zhou et al., 2018b). Chen (2014) found that 6 out of the 38 CMIP5 models, which can capture the interdecadal change of summer precipitation in eastern China, rely on reproducing the interdecadal weakening of the East Asian summer monsoon (EASM) circulations in the late 1970s. Gong et al. (2014) showed that poor simulations of the ENSO-East Asian winter monsoon (EAWM) relationship might limit the simulation of winter precipitation. In addition, the optimization of convective parameterization schemes has an important role in reducing model bias. The improvement of precipitation simulations from the CMIP3 to the CMIP5 is partly attributed to the enhanced simulation of convective precipitation due to the optimization of convective parameterization (Yuan, 2013; Wei et al., 2014). Simulation bias may also be related to the model resolution. Compared with the low-resolution models, the models with higher resolutions can improve the simulations of seasonal atmospheric circulations and consequently reduce the bias (Gao et al., 2006; Yao et al., 2017; Lin et al., 2018; Vannière et al., 2019; Bock et al., 2020).

Some studies have documented that the difference in the projected changes of the East Asian precipitation may arise from the discrepancies among models in the projection of changes in atmospheric circulations, such as the East Asian westerly jet and the western Pacific subtropical high (Ren et al., 2017; Zhou et al., 2018b, 2020; Tian et al., 2019). Li et al. (2019) revealed that the dynamic role associated with changes in monsoon circulations dominates the projected change of the EASM precipitation when the increase in global temperature exceeds 2°C. Nevertheless, Li et al. (2022) reported that the projected change in East Asian precipitation is mainly attributed to the thermodynamic role; the contribution from the dynamic role is weak.

Recently, CMIP6 analyses of precipitation in China have been gradually conducted (e.g., Chen et al., 2020; Jiang et al., 2020; Xin et al., 2020; Zhu et al., 2020; Yang et al., 2021). Based on the performance of 20 CMIP6 models in simulating the climatology and interannual variability of precipitation over China, Yang et al. (2021) grouped the models into three ensembles: the "highest-ranked" model ensemble (BMME), "lowest-ranked" model ensemble (WMME), and all-model ensemble (AMME) to project changes of precipitation in China under the SSP5-8.5 and SSP2-4.5 scenarios. The results indicated salient differences among the three ensembles in the simulation and projection of precipitation, particularly over northern China. However, the possible reasons for the differences were not examined. In this study, we extend their study to address this issue, focusing on the precipitation in northern China. Considering the larger projected precipitation changes over northern China under SSP5-8.5 than that under SSP2-4.5, we chose the SSP5-8.5 scenario to analyze the discrepancies among the three ensemble projections.

The remainder of this paper is organized as follows. Section 2 outlines the data and methods. Section 3 and Section 4 present the reasons for the discrepancies of precipitation simulation and projection in northern China among the three ensembles, respectively. The main findings are concluded in section 5.

2. Data and methods

2.1. *Datasets*

The outputs from the historical simulation (1995–2014) and the SSP5-8.5 experiment (2081–2100) of 20 CMIP6 models are used. The SSP5-8.5 represents a combined scenario of a high energy-intensive, socioeconomic developmental path (i.e., SSP5) with strong radiative forcing peaking at 8.5 W m^{-2} by 2100 (O'Neill et al., 2016). The 20 CMIP6 models used for the AMME and the models used for the BMME and WMME are shown in Table 1. The members selected for the BMME and WMME were based on their respective performances on the observed climatology and interannual variability of precipitation during 1995–2014. Further details are provided in Yang et al. (2021).

The CN05.1 precipitation data (Wu and Gao, 2013) and the ERA5 reanalysis data (Hersbach et al., 2020), each having a 0.25° × 0.25° resolution, are also employed (hereafter referred to as "observation"). The variables from the EAR5 reanalysis include evaporation (E), specific humidity (q), meridional wind (v), zonal wind (u), geopotential height (Z), sea level pressure (SLP), surface pressure (P_s), and vertical velocity (ω). Because of the varying resolutions of the data, we used the bilinear interpolation method to interpolate all the data to 1° × 1° grid resolution. To avoid artificial increases in geopotential height due to the influence of global warming (He et al., 2015; Huang et al., 2015, 2016; Zhang et al., 2021), the eddy geopotential height, defined as the departure from its zonal mean, was adopted for the analysis of projected changes.

2.2. *Methods*

We attempt to diagnose the cause for the differences among the three ensembles in the simulation and projection

Table 1. 20 CMIP6 models used for all-model ensemble (AMME) and the members (marked by √) used for "highest-ranked" model ensemble (BMME) and "lowest-ranked " model ensemble (WMME).

	DJF		JJA	
Model name	BMME	WMME	BMME	WMME
ACCESS-CM2			√	
ACCESS-ESM1-5				√
BCC-CSM2-MR			√	
CanESM5				
CESM2				√
CESM2-WACCM				
EC-Earth3	√			
EC-Earth3-Veg	√			
FGOALS-g3				√
GFDL-CM4	√			
GFDL-ESM4				
INM-CM4-8		√	√	
INM-CM5-0		√		
IPSL-CM6A-LR				
MIROC6				
MPI-ESM1-2-HR				
MPI-ESM1-2-LR		√		√
MRI-ESM2-0				
NorESM2-LM				
NorESM2-MM				

of winter (December to February, DJF) and summer (June to August, JJA) precipitation in terms of the atmospheric circulation and moisture budget. When considering precipitation climatology, moisture variation with time ($\partial_t \langle q \rangle$) is negligible (Bao and Feng, 2016; Li et al., 2017). Thus, the vertically integrated moisture equation is shown in Eq. (1) (Trenberth and Guillemot, 1995), which can be simplified by Eq. (2):

$$\partial_t \langle q \rangle = -P - \langle V_h \cdot \nabla_h q \rangle - \left\langle \omega \partial_p q \right\rangle + E + \mathrm{Res}\,, \tag{1}$$

$$P = -\langle V_h \cdot \nabla_h q \rangle - \left\langle \omega \partial_p q \right\rangle + E + \mathrm{Res}\,, \tag{2}$$

where the operator $\langle . \rangle = \frac{1}{g}\int_{P_s}^{100} \mathrm{d}p$, $-\langle V_h \cdot \nabla_h q \rangle$ and $-\left\langle \omega \partial_p q \right\rangle$ represent horizontal moisture advection and vertical moisture advection, respectively; E indicates evaporation, and Res is the residual term.

Referencing Chou et al. (2009), the moisture budget for the projected change of precipitation (dP) at the end of the 21st century (2081–2100) relative to the reference period (1995–2014) is estimated as:

$$\begin{aligned} \mathrm{d}P &= \mathrm{dTH} + \mathrm{dDY} + \mathrm{dNL} + \mathrm{d}E + \mathrm{Res} \\ \mathrm{dTH} &= -\left\langle \overline{\omega} \partial_p q' \right\rangle - \left\langle \overline{V}_h \cdot \nabla_h q' \right\rangle \\ \mathrm{dDY} &= -\left\langle \omega' \partial_p \overline{q} \right\rangle - \langle V'_h \cdot \nabla_h \overline{q} \rangle \\ \mathrm{dNL} &= -\left\langle \omega' \partial_p q' \right\rangle - \langle V'_h \cdot \nabla_h q' \rangle \end{aligned} \tag{3}$$

in which the overbar operator, $\overline{\ }$, is the climatology of the reference period and the prime operator, $'$, denotes the future change relative to the reference period; dTH, dDY, and dNL represent the thermodynamic contribution related to the change in specific humidity, the dynamic contribution associated with the change in atmospheric circulation, and the nonlinear term influenced by changes in both specific humidity and atmospheric circulation, respectively.

3. Simulation Bias

3.1. *Precipitation bias*

First, we present the biases of winter and summer precipitation as simulated by the three ensembles for 1995–2014. As shown in Fig. 1, the BMME outperforms the AMME and WMME in simulating the spatial pattern of observed winter precipitation. However, all the ensembles generally show an overestimation in northern China, especially in Northwest China (NWC, 36°–46°N, 75°–111°E). One exception is the presence of negative biases in Xinjiang for the BMME simulation (Fig. 1e), which differs from that simulated by the AMME (Fig. 1c) and WMME (Fig. 1g). For summer precipitation, the BMME simulation shows less improvement compared to the other two ensembles. Jiang et al. (2020) compared the performances of CMIP5 and CMIP6 models in capturing the climatological precipitation over China. Their study revealed that the performances have improved from the CMIP5 to the CMIP6. Lun et al. (2021) also indicated that the overestimation of precipitation is reduced from the CMIP5 to the CMIP6 in the ensemble of optimal models.

When regionally averaged, the BMME simulation exhibits the smallest deviation from the observation for both the winter and summer precipitation, followed by the AMME simulation and then the WMME simulation. Specifically, the percentage-based wet biases for winter (summer) precipitation over NWC, North China (NC, 36°–46°N, 111°–119°E), and Northeast China (NEC, 39°–54°N, 119°–134°E) in the BMME simulation are 462%, 185%, and 132% (51%, 25%, and 8%), which increase to 1433%, 267% and 187% (55%, 26%, and 15%) in the AMME simulation and further to 2763%, 473%, and 326% (78%, 27% and 16%) in the WMME simulation, respectively (Table 2). Note that larger percentage-based wet biases in winter compared to summer do not reflect the larger biases of the absolute values due to the different climatology of seasonal precipitation in northern China (Table 2).

3.2. *Atmospheric circulation bias*

Large-scale atmospheric circulations provide an important background for the occurrence of precipitation. In general, the precipitation in NWC is influenced by the westerly circulation, while precipitation over eastern China is primarily influenced by monsoon circulations. The EAWM circulations are characterized by the Siberian high and the Aleutian low in SLP, the prevalent northerly over eastern China in

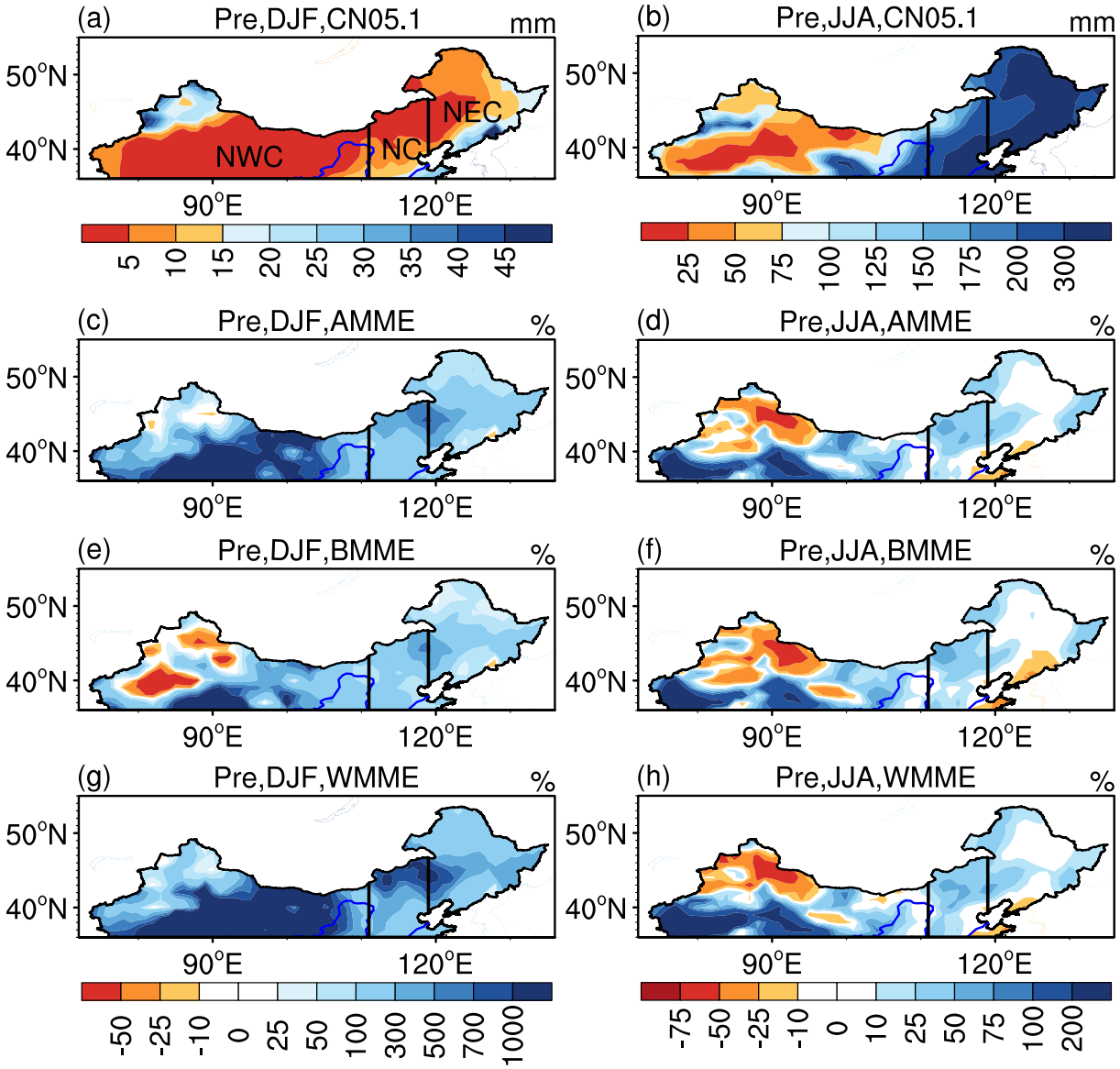

Fig. 1. Spatial distributions of (a, b) CN05.1 climatology (units: mm) and (c, d) AMME, (e, f) BMME, and (g, h) WMME simulation bias (units: %) for winter (left panel) and summer (right panel) precipitation during 1995–2014. The thick black lines represent the boundaries of subregions of northern China: Northeast China (NEC, 39°–54°N, 119°–134°E), North China (NC, 36°–46°N, 111°–119°E), and Northwest China (NWC, 36°–46°N, 75°–111°E).

Table 2. CN05.1 observed winter and summer precipitation (units: mm), and the AMME, BMME, and WMME simulated relative biases (units: %) and absolute biases (shown in parentheses; units: mm) over the subregions of northern China.

	Winter (DJF)				Summer (JJA)			
Subregion	Observation	AMME	BMME	WMME	Observation	AMME	BMME	WMME
NC	7	267 (18.69)	185 (12.95)	473 (33.11)	267	26 (69.42)	25 (66.75)	27 (72.09)
NEC	12	187 (22.44)	132 (15.84)	326 (39.12)	335	15 (50.25)	8 (26.8)	16 (53.6)
NWC	5	1433 (71.65)	462 (23.10)	2763 (138.15)	95	55 (52.25)	51 (48.45)	78 (74.10)

the lower troposphere (Fig. 2a), the East Asian trough in the middle troposphere, and the East Asian westerly jet in the upper troposphere (Fig. 2b). The EASM circulations are characterized by the prevailing southwesterly winds over eastern China in the lower troposphere (Fig. 3a), the western Pacific subtropical high in the middle troposphere, and the East Asian westerly jet, located around 40°N, in the upper troposphere (Fig. 3b).

The three ensembles can reasonably reproduce the basic features of the EAWM and EASM circulations. However, compared with observations, the AMME simulated SLP is slightly lower in the mid-high latitudes and higher

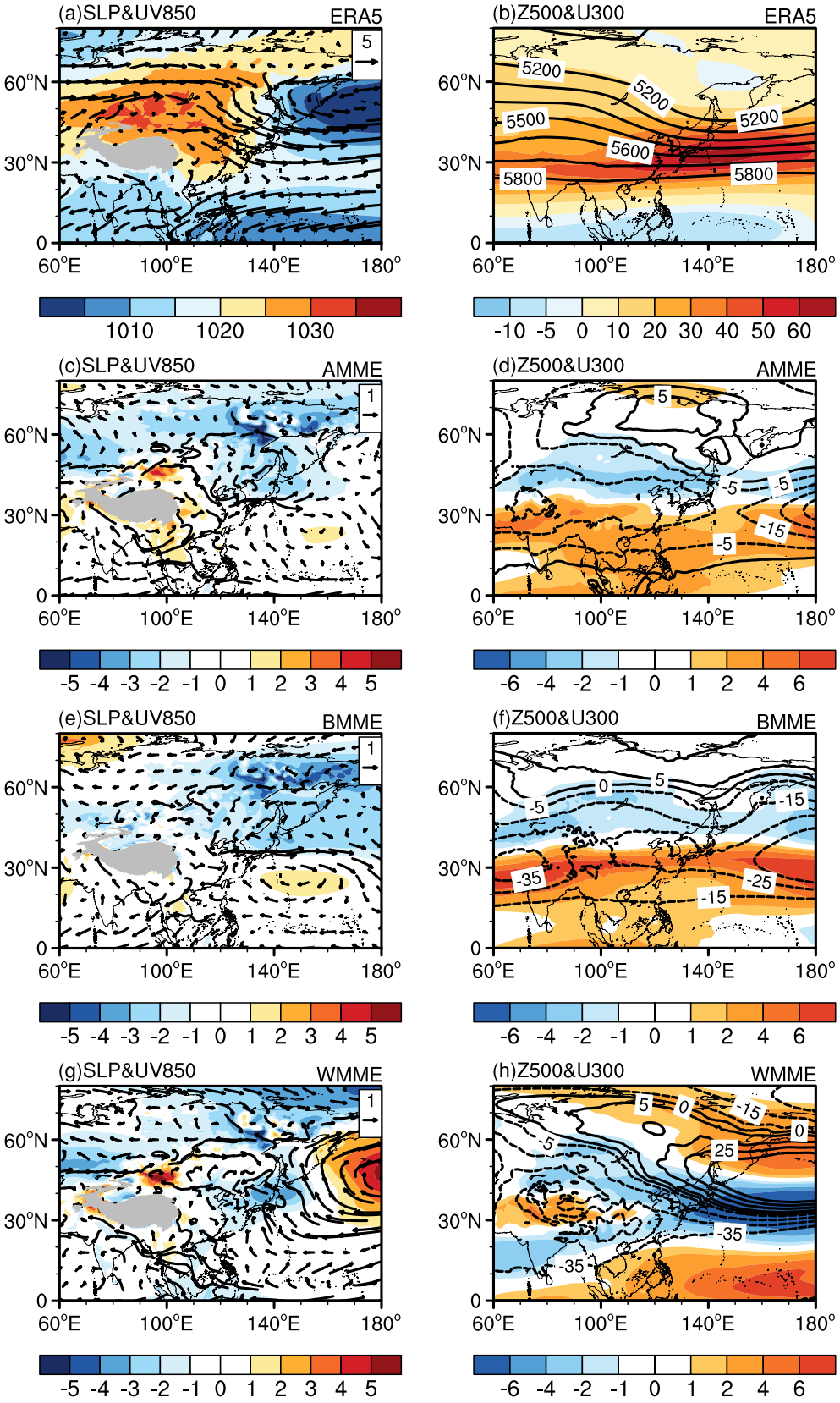

Fig. 2. Spatial distributions of (a, b) ERA5 climatology and simulation biases of (c, d) AMME, (e, f) BMME, and (g, h) WMME for (left panel) sea level pressure (shading; units: hPa) and 850 hPa winds (vectors; units: m s^{-1}) as well as (right panel) 500-hPa geopotential height (contours; units: gpm) and 300-hPa zonal wind (shading; units: m s^{-1}) during winters from 1995–2014. The gray shading represents the Tibetan Plateau.

around the Tibetan Plateau in winter (Fig. 2c), indicating an overestimation of the south-north meridional pressure gradient. Hence, a slightly stronger westerly flow is introduced, which contributes to a wet bias in NWC. The BMME simulated SLP is also somewhat lower in the mid-high latitudes; however, the positive SLP bias around the Tibetan Plateau is reduced compared to the AMME simulation (Fig. 2e). Thus, the westerly deviation simulated by the BMME is smaller than that of the AMME, reducing the wet bias over NWC in the BMME simulation. In the middle and high troposphere, a widespread negative bias in the 500-hPa geopotential height and a southward shift of the East Asian westerly jet are produced in the AMME and BMME (Figs. 2d, f). The WMME simulation bias behaves differently from that

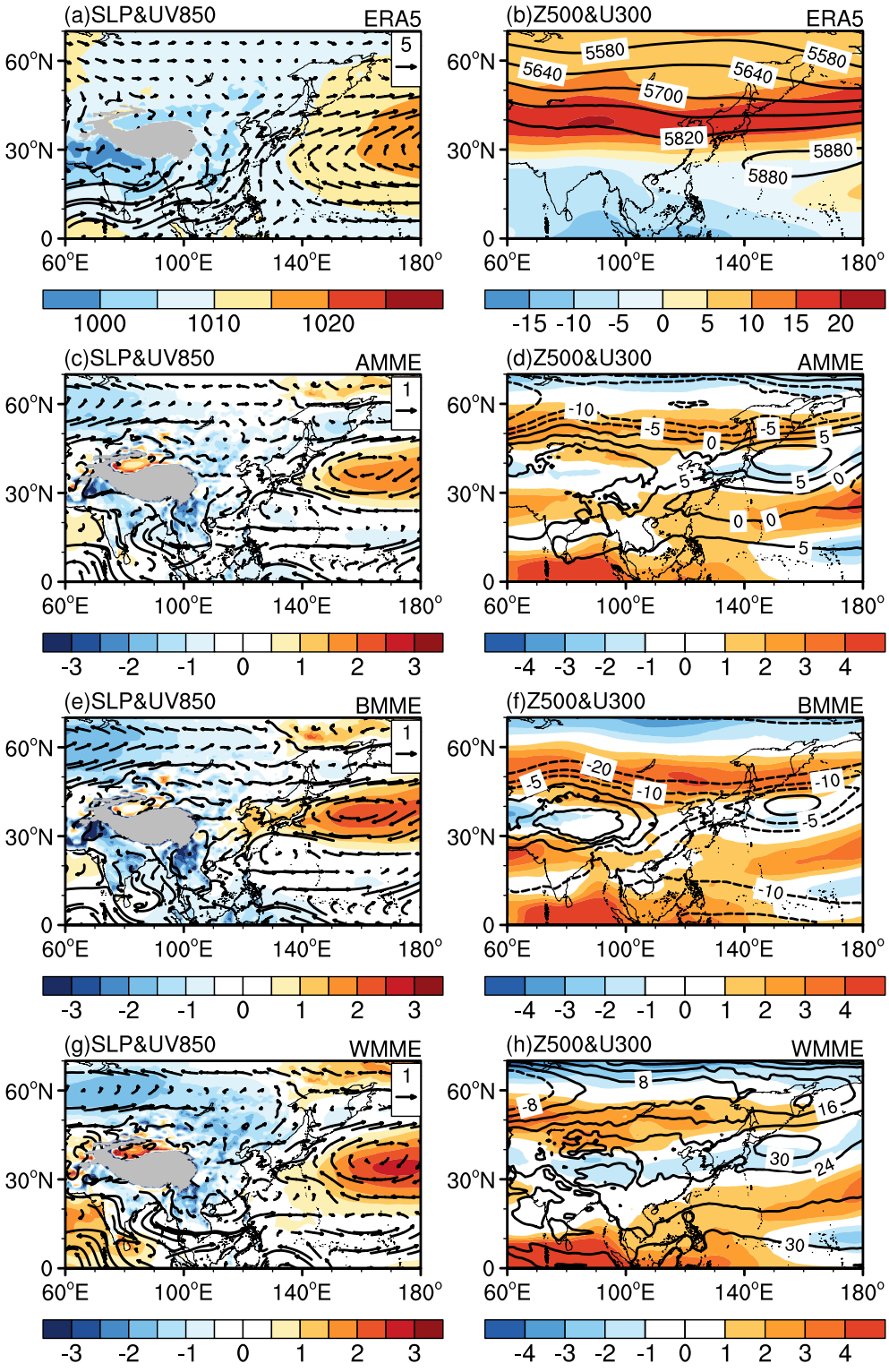

Fig. 3. Same as Fig. 2, but for summer.

of the AMME and BMME. For the WMME simulation (Figs. 2g, h), the simulated Aleutian low, East Asian trough, and East Asian westerly jet are consistently weaker than the observation. The biases in the EAWM circulations are significantly larger than that simulated by the AMME and BMME, making the WMME performance on winter precipitation inferior to that of the AMME and BMME.

During the summer, all the ensembles simulate an increased mid-latitude zonal pressure gradient, which allows for anomalous southwesterlies or westerlies to occur in the eastern part of northern China (Figs. 3c, e, g). The northwestern part of northern China is dominated by westerly anomalies. In addition, cyclonic and anticyclonic circulation anomalies at 850 hPa are prevalent to the south and north of 30°N in the western Pacific, respectively (Figs. 3c, e, g), indicating a relatively northward location of the western Pacific subtropical high. For the 500-hPa geopotential height, there are negative biases in the AMME and BMME simulations over the region where the observed 5880-gpm contour that characterizes the intensity of the western Pacific subtropical high is located (Figs. 3d, f). In contrast, a systematic positive bias is noted in the WMME simulation, indicating an overestimation of the western Pacific subtropical high (Fig. 3h). In the upper troposphere (Figs. 3d, f, h), the simulated zonal wind increases north of 40°N and weakens south of 40°N, suggesting a northward displacement of the East Asian westerly jet, which is conducive to the excessive precipitation in northern China (Lu, 2004; Huang et al., 2013; Ren et al., 2017; Zhou et al., 2018a). The BMME simulation for the upper-tropospheric zonal winds is generally similar to that of the AMME and WMME, which is partly responsible for the fact that the BMME simulated summer precipitation is not saliently improved.

3.3. *Moisture budget bias*

Figure 4a shows the observed climatological values for the winter moisture budget terms in each of the subregions (NWC, NC, NEC) of northern China. The results indicate that all three subregions are characterized by the outward transport of moisture in winter, mainly due to the influence of the vertical moisture advection, and that the evaporation is balanced by precipitation. For the AMME simulation of

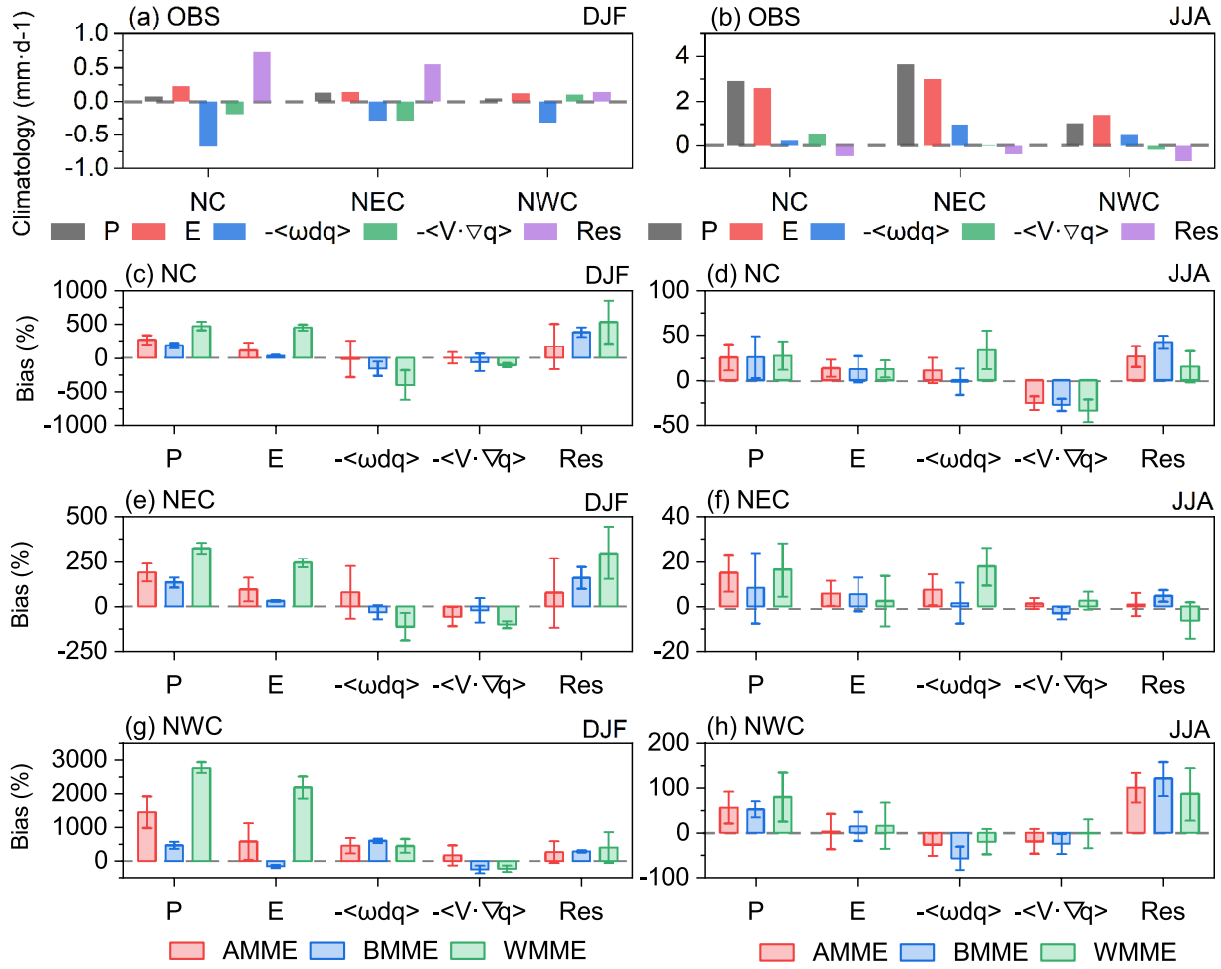

Fig. 4. Climatology of the observed (a) winter and (b) summer moisture budget (units: mm d^{-1}) in the three subregions of northern China during 1995–2014 and (c–h) simulation biases of AMME, BMME, and WMME for (left panels) winter and (right panels) summer moisture budget (units: %, percentage anomalies relative to 1995–2014). The boxes and error bars indicate the ensemble mean and the range of ±0.5 standard deviations, respectively.

winter precipitation in NWC (Fig. 4g), the wet bias mainly comes from the overestimation of the evaporation (571%) and vertical moisture advection (445%). The simulated evaporation bias in the WMME increases to 2160%, while it decreases to –162% in the BMME. In contrast, the bias of the simulated vertical moisture advection is comparable among the three ensembles. This means that different behaviors of the BMME, AMME, and WMME in simulating winter precipitation over NWC are mainly attributed to their simulated biases in evaporation.

Similarly, the overestimation of the evaporation also contributes to the wet biases of winter precipitation in NC and NEC. Among the three ensembles, the BMME presents the smallest evaporation biases (29% and 29%) in both NC and NEC, which increase to 112% and 93% in the AMME simulation and are further exaggerated to 451% and 242% in the WMME simulation, respectively (Figs. 4c, e). The BMME simulated advection of vertical and horizontal moisture is improved in NEC compared with the simulations of the AMME and WMME (Fig. 4e). It is worth noting that the residual term is somewhat large in NC and NEC (Figs. 4a, c, e), which may be a consequence of the sub-monthly transient eddies and the moisture imbalance between the models and the reanalysis, leaving the moisture budget analysis in these regions subject to a certain degree of uncertainty.

Figure 4b indicates that the contribution to the observed summer precipitation in NC (NEC and NWC) is mainly from the evaporation, followed by the horizontal moisture advection (vertical moisture advection). For simulations in NWC (Fig. 4h), the AMME, BMME, and WMME show biases of 2%, 14%, and 15% for the evaporation, –27%, –57%, and –20% for the vertical moisture advection, and –19%, –25%, and –2% for the horizontal moisture advection, respectively. Compared with the AMME and WMME, the BMME does not show notable improvement in the simulation of any given terms. Thus, the slight improvement of the BMME simulation for summer precipitation over this region is considered to be the result of a mutual offset between the overestimation and underestimation.

For the simulations in NC (NEC) (Figs. 4d, f), the evaporation biases of 13%, 12%, and 13% (6%, 5%, and 2%), respectively, from the AMME, BMME, and WMME are approximately the same. The biases of the simulated horizontal moisture advection among the three ensembles are also comparable. The slight improvement from the WMME to the BMME in simulating summer precipitation is mainly reflected in the enhancement of the performance on the vertical moisture advection. Compared with the WMME bias of 34% (18%) for the vertical moisture advection in NC (NEC), the bias decreases to 11% (7%) in the AMME simulation and decreases further to –2% (1%) in the BMME simulation.

In brief, the wet winter bias in northern China in the three ensembles mainly results from overestimating the evaporation. Due to a significant reduction of the evaporation bias in the BMME, it performs better than the AMME and WMME in reproducing winter precipitation over northern China. In contrast, the enhancement of the BMME performance on the vertical moisture advection contributes to reducing the wet summer bias in NC and NEC.

4. Projected Change

4.1. *Precipitation change*

Figure 5 displays the projected percentage changes in winter and summer precipitation over northern China at the end of the 21st century under SSP5-8.5. In winter (Figs. 5a–c), the precipitation is projected to increase across northern China, with the greatest increase in the BMME, followed by the AMME and then the WMME. The average precipitation increases for the BMME, AMME, and WMME projections

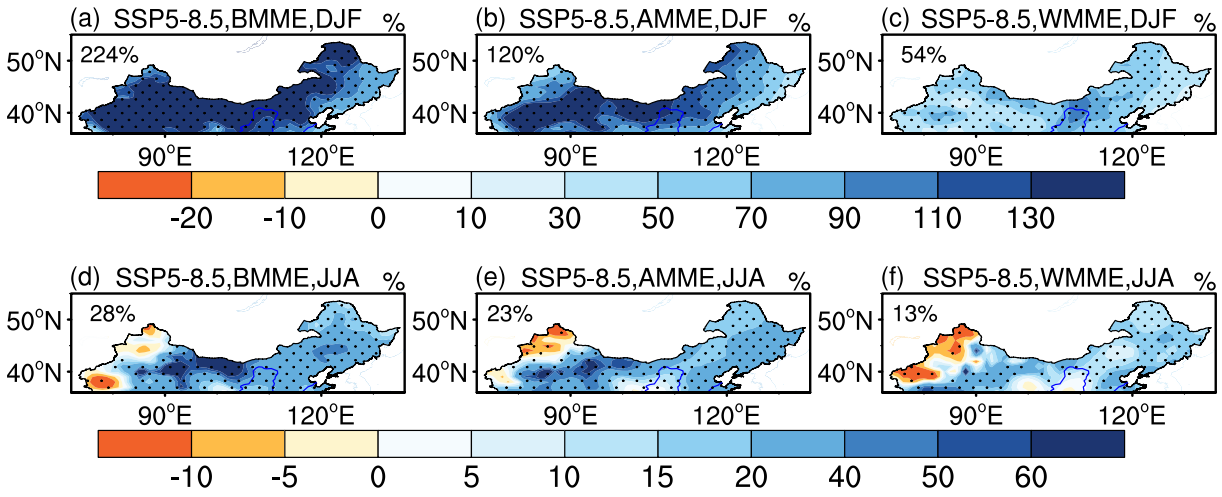

Fig. 5. Projected percentage changes in (a–c) winter and (d–f) summer precipitation (units: %) under SSP5-8.5 over the period 2081–2100 relative to 1995–2014 from (a, d) BMME, (b, e) AMME, and (c, f) WMME. The values in the upper-left corner indicate the regional average over Northern China. Black solid dots represent grids with a statistically significant change at the 95% confidence level.

are 224%, 120%, and 54%, respectively. It reflects the uncertainty in the magnitudes of projected changes in winter precipitation for different ensemble projections. The summer precipitation is also projected to increase in northern China, except that a decrease is projected in the western part of NWC. The BMME projected increase averaged over northern China is 28%, larger than that of the AMME (23%) and WMME (13%) (Figs. 5d–f). Similar results can be obtained when averaged over the subregions.

4.2. *Atmospheric circulation change*

Figure 6 shows the changes in large-scale atmospheric circulations during the winter season as projected by the three ensembles. In the lower troposphere (Figs. 6a–c), all the three ensembles project an anomalous anticyclonic circulation and an anomalous cyclonic circulation, respectively, residing in the southern and northern flanks of the North Pacific, indicating a northward shift of the Aleutian low. The anticyclonic circulation anomaly weakens the climatological northerly winds in the reference period and facilitates the northward transport of moisture from the south. This result is consistent with the findings in CMIP3 and CMIP5 studies (Jiang and Tian, 2013; Hong et al., 2017). In the middle troposphere, the eddy geopotential height increases over the region where the East Asian trough is located, indicating a weakening of the East Asian trough. Concurrently, the East Asian westerly jet in the upper troposphere is projected to shift northward (Figs. 6d–e). Compared with the AMME projection, the BMME (WMME) projected magnitudes of changes are larger (smaller).

In summer, the projected atmospheric circulation changes from the three ensembles are similar. An increase (decrease) in SLP accompanied by an anomalous anticyclonic (cyclonic) circulation at 850 hPa is projected in the Indian Ocean and South China Sea (East Asia), which tends to drive the northward transport of moisture from the ocean (Figs. 7a–c). In the middle troposphere (Figs. 7d–f), negative eddy geopotential height anomalies are projected in the western North Pacific, which conforms to the CMIP5 projection and indicates a weakening of the western Pacific subtropical high (He et al., 2015). In the upper troposphere (Figs. 7d–f), the easterly anomalies and westerly anomalies prevail north and south 40°N, respectively, indicating a southward shift of the East Asian westerly jet.

4.3. *Moisture budget changes*

We quantified the future projected changes of the winter and summer moisture budgets over the three subregions during 2081–2100, referenced from 1995–2014. As shown in Fig. 8, change in evaporation (dE) positively contributes to increases in both winter and summer precipitation in northern China; the change in the thermodynamic component (dTH) negatively contributes to the increases in winter precipitation in NC and NEC and summer precipitation in NC and NWC; the change in dynamic component (dDY) shows a positive contribution to the increases of winter precipitation in NC and NWC and summer precipitation in NC and NEC; the change in the nonlinear term (dNL) generally shows positive

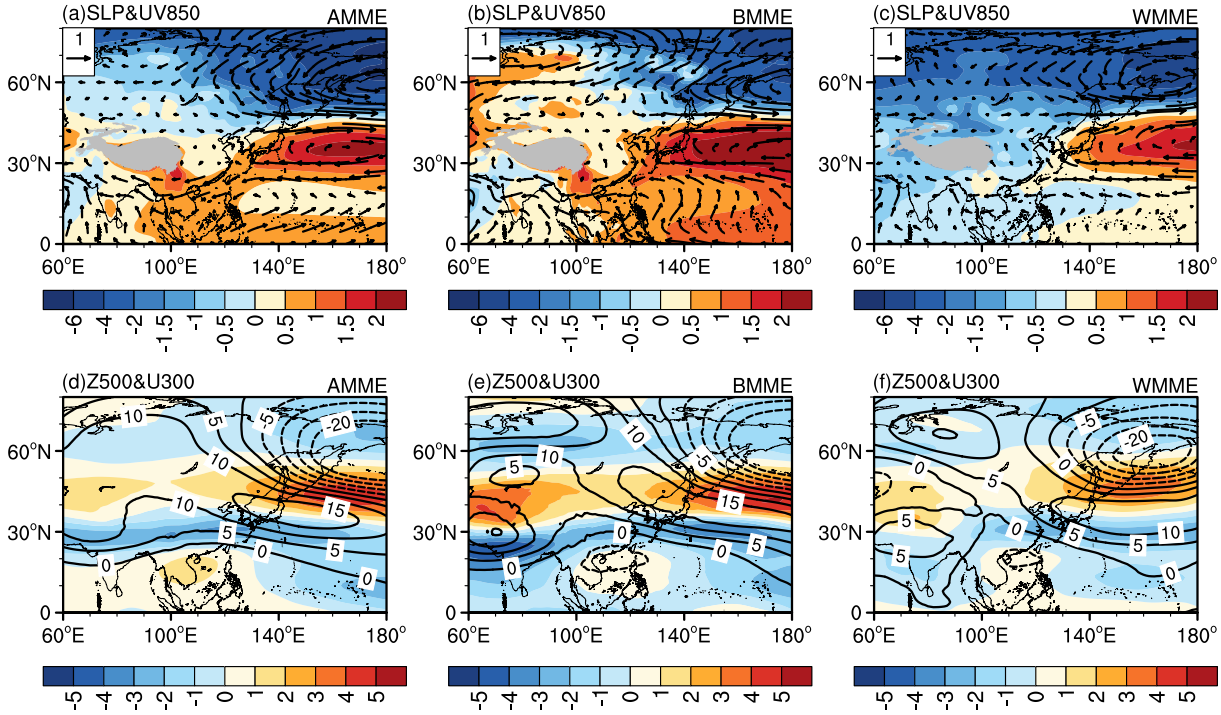

Fig. 6. (a, d) AMME, (b, e) BMME, and (c, f) WMME projected changes in (a–c) sea level pressure (shading; units: hPa) and 850 hPa winds (vectors; units: m s^{-1}) as well as (d–f) 500-hPa eddy geopotential height (contours; units: gpm) and 300-hPa zonal wind (shading; units: m s^{-1}) under SSP5-8.5 in winter during 2081–2100 relative to the reference period, 1995–2014. The gray shading represents the Tibetan Plateau.

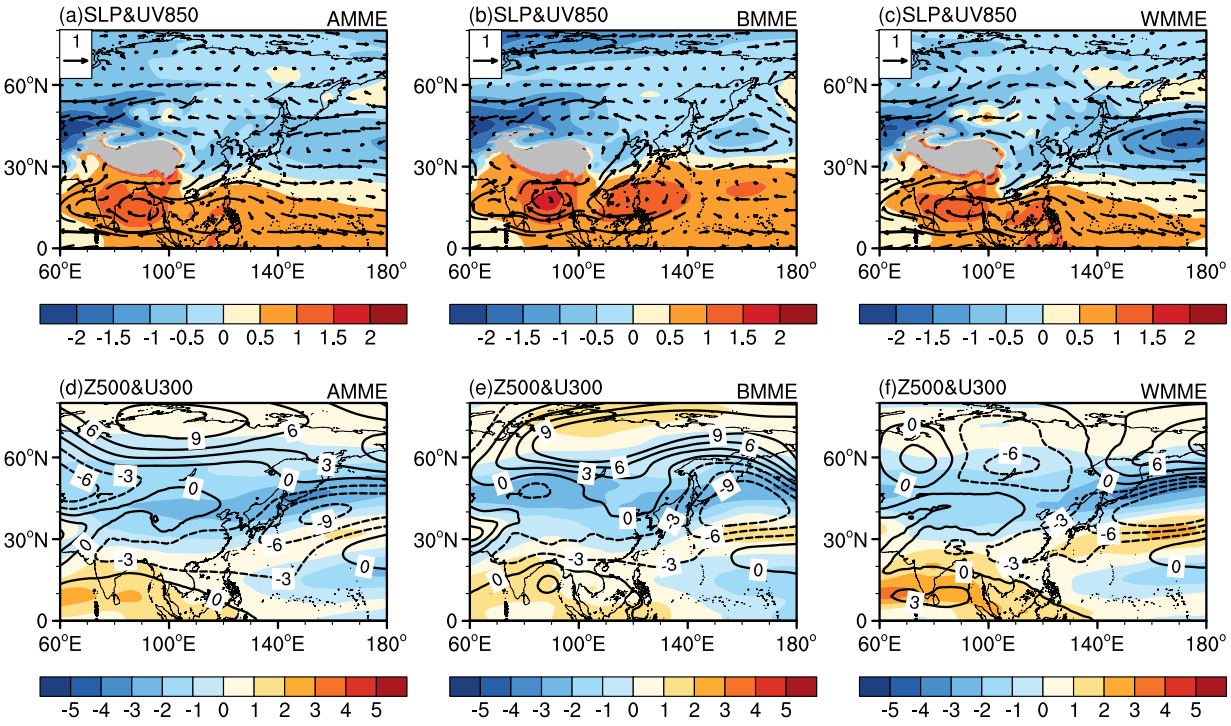

Fig. 7. Same as Fig. 6, but for summer.

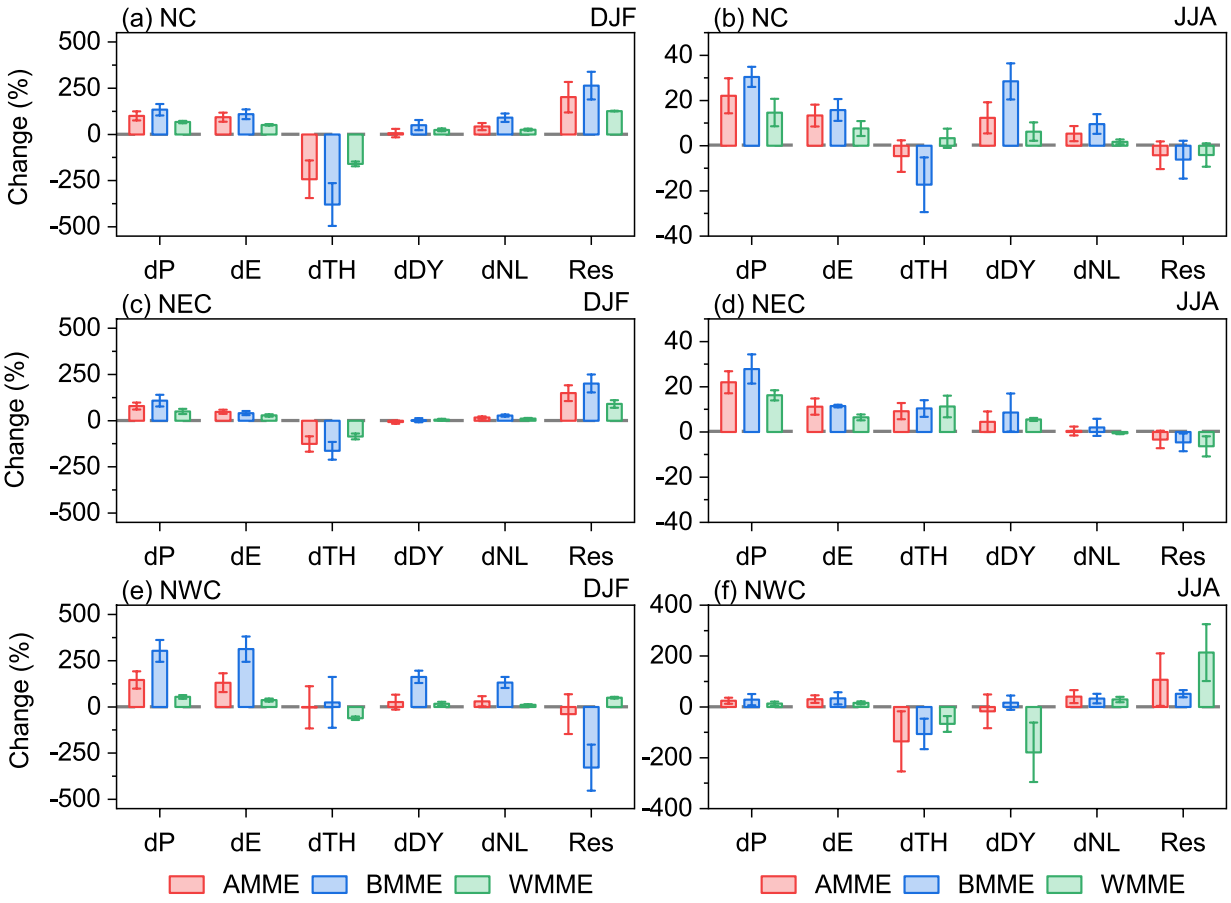

Fig. 8. AMME, BMME, and WMME projected changes of (left panel) winter and (right panel) summer moisture budget in (a, b) North China, (c, d) Northeast China, and (e, f) Northwest China during 2081–2100 relative to the reference period 1995–2014 (units: %). Boxes and error bars represent the ensemble mean and ±0.5 standard deviations, respectively.

contribution.

By comparing the projections of three ensembles, we can notice that the projected magnitudes of the changes in winter evaporation increase from the WMME to the BMME, which accounts for larger increases in winter precipitation from the WMME to the BMME in each subregion (Figs. 8a, c, e). Among the three ensembles, the WMME projects the smallest increase of evaporation in NWC (37%), NC (51%), and NEC (28%), contributing to the smallest increase of winter precipitation in situ. The AMME (BMME) projected changes in winter evaporation are much larger, with an increase of 131%, 93%, and 47% (313%, 109%, and 41%) in NWC, NC, and NEC, respectively. The increase of the nonlinear component also plays a role in the projected increase in the magnitude of winter precipitation from the WMME to the BMME. In addition, a larger change in the dynamic component, as projected by the BMME, contributes to larger increases in winter precipitation in NC and NWC.

The increasing magnitude of projected changes in summer evaporation also contributes to the enhancement of summer precipitation from the WMME to the BMME (Figs. 8b, d, f). For the WMME projection, the evaporation increases by 8%, 6%, and 15% in NC, NEC, and NWC, respectively. The counterparts are further enhanced to 16%, 11%, and 34% in the BMME projection. Additionally, larger increases in summer precipitation are associated with higher dynamic contributions. The BMME projected dynamical contribution increases by 28% in NC, 9% in NEC, and 17% in NWC, while the corresponding changes in the AMME (WMME) projection are 12%, 5%, and –18% (6%, 17%, and –179%), respectively.

In general, the warming of surface air temperature (Yang et al., 2021) favors the evaporation process, allowing the evaporation to positively contribute to the precipitation increase in northern China. Using the moisture budget equation, Endo and Kitoh (2014) diagnosed the CMIP5 multimodel ensemble projected change of summer precipitation in the East Asian monsoon region south of 40°N under RCP8.5. They revealed that the increase in precipitation is mainly due to the increases in evaporation and in the thermodynamic contribution. However, our study finds that the thermodynamic factor generally signals a negative contribution in northern China. Instead, the increases in evaporation and the dynamic contribution are responsible for the BMME projected larger increase in precipitation (Fig. 8). As seen in Fig. 9, anomalous vertical upward motion is projected to occur over northern China in both winter and summer, which can explain the precipitation change resulting from the dynamic or nonlinear contribution. In particular, the projected stronger ascending anomaly by the BMME, compared

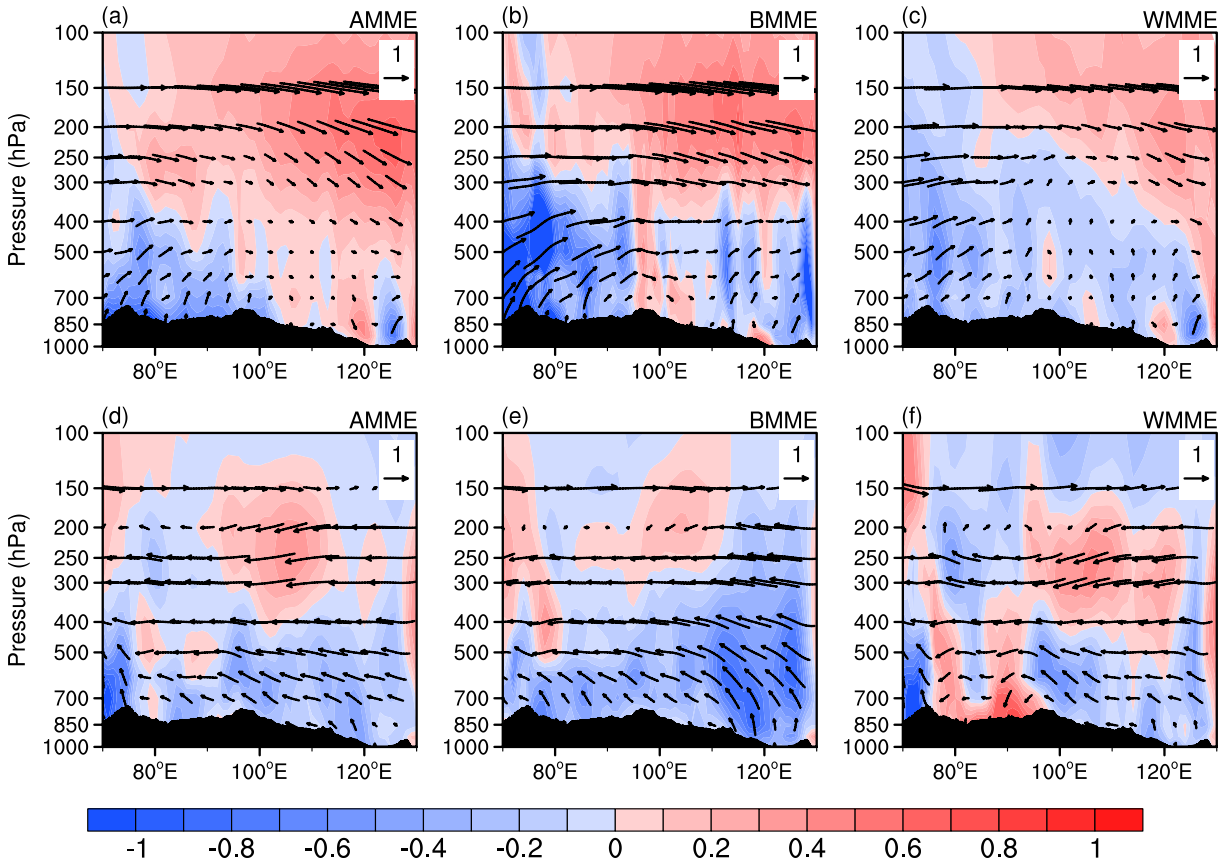

Fig. 9. (a, d) AMME, (b, e) BMME, and (c, f) WMME projected changes in the zonal wind (vectors; units: m s^{-1}) and vertical velocity (shading; units: 10^{-2} Pa s^{-1}) averaged over 36°–46°N in (a–c) winter and (d–f) summer under SSP5-8.5 during 2081–2100 relative to the reference period 1995–2014. Black shading denotes mountains.

to the AMME and WMME projections, can also explain why the BMME projects more precipitation in northern China during the winter and summer seasons.

5. Conclusion

The comparison of the BMME, AMME, and WMME biases indicates that the BMME outperforms the AMME and WMME in the simulation of winter precipitation and shows a slight improvement in the simulation of summer precipitation over northern China. For winter precipitation, the BMME simulated percentage deviations from the observation are 462%, 185%, and 132% in NWC, NC, and NEC, respectively, which are much lower than those in the AMME (1433%, 267%, and 187%) and WMME (2763%, 473%, and 326%) simulations. For summer precipitation, the wet biases in NWC, NC, and NEC from the BMME are 51%, 25%, and 8%, while those in the AMME (WMME) simulation are 55%, 26%, and 15% (78%, 27%, and 16%), respectively. Relative to the reference period 1995–2014, the winter and summer precipitation in northern China are projected to increase at the end of the 21st century under SSP5-8.5, with a larger increase in the BMME projection compared to those in the AMME and WMME projections. The possible reasons underlying such discrepancies are explored in terms of large-scale atmospheric circulations and moisture budget. The main findings are summarized as follows:

(1) The three ensembles can capture the basic characteristics of the EAWM and EASM circulations. However, compared to observations, the WMME simulated winter Aleutian low, western Pacific subtropical high, and East Asian westerly jet are consistently weaker, while the BMME and AMME simulated EAWM circulations are better matched with the observations. The simulation biases for the EASM circulations from the three ensembles are generally similar, with a stronger mid-latitude zonal pressure gradient and a northward shift of the western Pacific subtropical high and the East Asian westerly jet. However, the WMME overestimates the intensity of the western Pacific subtropical high when compared with the AMME and BMME.

(2) The moisture budget analysis indicates that the wet bias of the simulated winter precipitation is mainly related to the overestimation of evaporation. Among the three ensembles, the BMME shows the smallest evaporation bias, and the WMME shows the largest evaporation bias, which accounts for the reduction of the wet bias in northern China from the WMME to the BMME. The evaporation bias may be related to factors such as temperature, specific humidity, wind speed, and net surface radiation (Peng and Zhou, 2017), which deserves further investigation. Note that the residual term is somewhat large in NC and NEC, possibly resulting in a certain degree of uncertainty in the moisture budget. The simulated summer wet bias in North and Northeast China is mainly associated with the bias in simulating the evaporation and vertical moisture advection. The reduction in the BMME bias for the simulation of the vertical moisture advection contributes to its slight improvement for the simulation of summer precipitation in these two regions.

(3) Concerning future changes, the three ensembles project a northward shift of the Aleutian low, a weakening of the East Asian trough, and a northward shift of the East Asian westerly jet during the winter season of 2081–2100, with a larger change in the BMME projection than that in the AMME and WMME projections. The projected changes in summer atmospheric circulations from the three ensembles are similar, characterized by an increase in the south-north meridional pressure gradient between the ocean and the continent, a weakening of the western Pacific subtropical high, and a southward shift of the East Asian westerly jet.

(4) Evaporation changes positively contribute to the projected increases in both winter and summer precipitation in northern China. Compared to the WMME projection, the BMME projected increase in evaporation is much larger. The BMME projected higher dynamic contribution also accounts for larger increases in summer precipitation in northern China and winter precipitation in NC and NWC. In addition, the nonlinear component plays a role in the increasing magnitude of projected changes in winter precipitation from the WMME to the BMME. However, diversity exists in the thermodynamic contribution to the precipitation change over the subregions of northern China.

Overall, the results reported in our study are expected to deepen the understanding of the precipitation biases of CMIP6 models in northern China and provide a clue for the development of climate models. For instance, considering that the precipitation bias is closely linked to the evaporation bias, the improvement in the representation of precipitation-evaporation coupling in climate models may help to effectively improve model performance regarding precipitation in northern China. These findings also encourage better cognition of the uncertainty of projected climate change. Although a general increase in precipitation is projected in northern China, the magnitudes of the projected increases are different for different ensemble projections. Moreover, the large winter precipitation biases may also impose further uncertainty upon the conclusion, even if using the BMME, which could provide more reliable climate change signals. Note that this study focuses on the large-scale atmospheric circulations and moisture budget. Due to the complexity of the climate system, other factors may also contribute to the simulation and projection differences of seasonal precipitation among the three ensembles, which needs further examination. In addition, no one model in the BMME can simultaneously perform better for both winter and summer precipitation. Thus, more efforts are also needed to resolve this issue.

Acknowledgements. We acknowledge the World Climate Research Program's Working Group on Coupled Modeling and thank climate modeling groups for producing and sharing their model outputs. This research was jointly supported by the National Natural Science Foundation of China (Grant No. 41991285), the National Key Research and Development Program of China

(2017YFA0605004), and the Program for Distinguished Professors of Jiangsu.

REFERENCES

Bao, J. W., and J. M. Feng, 2016: Intercomparison of CMIP5 simulations of summer precipitation, evaporation, and water vapor transport over Yellow and Yangtze River basins. *Theor. Appl. Climatol.*, **123**, 437–452, https://doi.org/10.1007/s00704-014-1349-y.

Bock, L., and Coauthors, 2020: Quantifying progress across different CMIP phases with the ESMValTool. *J. Geophys. Res.: Atmos.*, **125**, e2019JD032321, https://doi.org/10.1029/2019JD032321.

Chen, H., 2014: Validation of the CMIP5 climate models in simulating decadal variations of summer rainfall in eastern China. *Climatic and Environmental Research*, **19**, 773–786, https://doi.org/10.3878/j.issn.1006-9585.2014.13174. (in Chinese with English abstract)

Chen, H. P., and J. Q. Sun, 2013: Projected change in East Asian summer monsoon precipitation under RCP scenario. *Meteorol. Atmos. Phys.*, **121**, 55–77, https://doi.org/10.1007/s00703-013-0257-5.

Chen, H. P., J. Q. Sun, W. Q. Lin, and H. W. Xu, 2020: Comparison of CMIP6 and CMIP5 models in simulating climate extremes. *Science Bulletin*, **65**, 1415–1418, https://doi.org/10.1016/j.scib.2020.05.015.

Chou, C. A., J. D. Neelin, C.-A. Chen, and J.-Y. Tu, 2009: Evaluating the "rich-get-richer" mechanism in tropical precipitation change under global warming. *J. Climate*, **22**, 1982–2005, https://doi.org/10.1175/2008JCLI2471.1.

Endo, H., and A. Kitoh, 2014: Thermodynamic and dynamic effects on regional monsoon rainfall changes in a warmer climate. *Geophys. Res. Lett.*, **41**, 1704–1711, https://doi.org/10.1002/2013GL059158.

Gao, X. J., Y. Xu, Z. C. Zhao, J. S. Pal, and F. Giorgi, 2006: On the role of resolution and topography in the simulation of East Asia precipitation. *Theor. Appl. Climatol.*, **86**, 173–185, https://doi.org/10.1007/s00704-005-0214-4.

Gong, H. N., L. Wang, W. Chen, R. G. Wu, K. Wei, and X. F. Cui, 2014: The climatology and interannual variability of the East Asian winter monsoon in CMIP5 models. *J. Climate*, **27**, 1659–1678, https://doi.org/10.1175/JCLI-D-13-00039.1.

He, C., T. J. Zhou, A. L. Lin, B. Wu, D. J. Gu, C. H. Li, and B. Zheng, 2015: Enhanced or weakened western North Pacific subtropical high under global warming? *Scientific Reports*, **5**, 16771, https://doi.org/10.1038/srep16771.

Hersbach, H., and Coauthors, 2020: The ERA5 global reanalysis. *Quart. J. Roy. Meteor. Soc.*, **146**, 1999–2049, https://doi.org/10.1002/qj.3803.

Hong, J. Y., J. B. Ahn, and J. G. Jhun, 2017: Winter climate changes over East Asian region under RCP scenarios using East Asian winter monsoon indices. *Climate Dyn.*, **48**, 577–595, https://doi.org/10.1007/s00382-016-3096-5.

Hu, T., Y. Sun, and X. B. Zhang, 2017: Temperature and precipitation projection at 1. 5 and 2°C increase in global mean temperature. *Chinese Science Bulletin*, **62**, 3098–3111, https://doi.org/10.1360/N972016-01234. (in Chinese with English abstract)

Huang, D. Q., J. Zhu, Y. C. Zhang, and A. N. Huang, 2013: Uncertainties on the simulated summer precipitation over eastern China from the CMIP5 models. *J. Geophys. Res.: Atmos.*, **118**, 9035–9047, https://doi.org/10.1002/jgrd.50695.

Huang, Y. Y., X. F. Li, and H. J. Wang, 2016: Will the western Pacific subtropical high constantly intensify in the future? *Climate Dyn.*, **47**, 567–577, https://doi.org/10.1007/s00382-015-2856-y.

Huang, Y. Y., H. J. Wang, K. Fan, and Y. Q. Gao, 2015: The western Pacific subtropical high after the 1970s: Westward or eastward shift? *Climate Dyn.*, **44**, 2035–2047, https://doi.org/10.1007/s00382-014-2194-5.

Jiang, D. B., and Z. P. Tian, 2013: East Asian monsoon change for the 21st century: Results of CMIP3 and CMIP5 models. *Chinese Science Bulletin*, **58**, 1427–1435, https://doi.org/10.1007/s11434-012-5533-0.

Jiang, D. B., D. Hu, Z. P. Tian, and X. M. Lang, 2020: Differences between CMIP6 and CMIP5 models in simulating climate over China and the East Asian monsoon. *Adv. Atmos. Sci.*, **37**, 1102–1118, https://doi.org/10.1007/s00376-020-2034-y.

Jiang, D. B., Z. P. Tian, and X. M. Lang, 2016: Reliability of climate models for China through the IPCC Third to Fifth Assessment Reports. *International Journal of Climatology*, **36**, 1114–1133, https://doi.org/10.1002/joc.4406.

Kumar, D., E. Kodra, and A. R. Ganguly, 2014: Regional and seasonal intercomparison of CMIP3 and CMIP5 climate model ensembles for temperature and precipitation. *Climate Dyn.*, **43**, 2491–2518, https://doi.org/10.1007/s00382-014-2070-3.

Li, J., Y. Zhao, D. L. Chen, Y. Z. Kang, and H. Wang, 2022: Future precipitation changes in three key sub-regions of East Asia: The roles of thermodynamics and dynamics. *Climate Dyn.*, **59**, 1377–1398, https://doi.org/10.1007/s00382-021-06043-w.

Li, P. X., T. J. Zhou, L. W. Zou, X. L. Chen, W. X. Zhang, and Z. Guo, 2017: Simulation of climatology and interannual variability of spring persistent rains by MRI model: Comparison of different horizontal resolutions. *Chinese Journal of Atmospheric Science*, **41**, 515–532, https://doi.org/10.3878/j.issn.1006-9895.1606.16151. (in Chinese with English abstract)

Li, Z. B., Y. Sun, T. M. Li, Y. H. Ding, and T. Hu, 2019: Future changes in East Asian summer monsoon circulation and precipitation under 1.5 to 5°C of warming. *Earth's Future*, **7**, 1391–1406, https://doi.org/10.1029/2019EF001276.

Lin, C. G., D. L. Chen, K. Yang, and T. H. Ou, 2018: Impact of model resolution on simulating the water vapor transport through the central Himalayas: Implication for models' wet bias over the Tibetan Plateau. *Climate Dyn.*, **51**, 3195–3207, https://doi.org/10.1007/s00382-018-4074-x.

Lu, R. Y., 2004: Associations among the components of the East Asian summer monsoon system in the meridional direction. *J. Meteor. Soc. Japan Ser. II*, **82**, 155–165, https://doi.org/10.2151/jmsj.82.155.

Lu, X., X. Q. Rao, and W. J. Dong, 2021: Model evaluation and uncertainties in projected changes of drought over northern China based on CMIP5 models. *International Journal of Climatology*, **41**, E3085–E3100, https://doi.org/10.1002/joc.6907.

Lun, Y. R., L. Liu, L. Cheng, X. P. Li, H. Li, and Z. X. Xu, 2021: Assessment of GCMs simulation performance for precipitation and temperature from CMIP5 to CMIP6 over the Tibetan Plateau. *International Journal of Climatology*, **41**, 3994–4018, https://doi.org/10.1002/joc.7055.

Niu, X. R., and Coauthors, 2015: Multimodel ensemble projection

of precipitation in eastern China under A1B emission scenario. *J. Geophys. Res.: Atmos.*, **120**, 9965–9980, https://doi.org/10.1002/2015JD023853.

O'Neill, B. C., and Coauthors, 2016: The Scenario Model Intercomparison Project (ScenarioMIP) for CMIP6. *Geoscientific Model Development*, **9**, 3461–3482, https://doi.org/10.5194/gmd-9-3461-2016.

Peng, D. D., and T. J. Zhou, 2017: Why was the arid and semiarid northwest China getting wetter in the recent decades? *J. Geophys. Res.: Atmos.*, **122**, 9060–9075, https://doi.org/10.1002/2016JD026424.

Rao, X. Q., X. Lu, and W. J. Dong, 2019: Evaluation and projection of extreme precipitation over Northern China in CMIP5 Models. *Atmosphere*, **10**, 691, https://doi.org/10.3390/atmos10110691.

Ren, Y. J., B. T. Zhou, L. C. Song, and Y. Xiao, 2017: Interannual variability of western North Pacific subtropical high, East Asian jet and East Asian summer precipitation: CMIP5 simulation and projection. *Quaternary International*, **440**, 64–70, https://doi.org/10.1016/j.quaint.2016.08.033.

Sun, Q. H., C. Y. Miao, and Q. Y. Duan, 2015: Comparative analysis of CMIP3 and CMIP5 global climate models for simulating the daily mean, maximum, and minimum temperatures and daily precipitation over China. *J. Geophys. Res.: Atmos.*, **120**, 4806–4824, https://doi.org/10.1002/2014JD022994.

Tian, D., Y. Guo, and W. J. Dong, 2015: Future changes and uncertainties in temperature and precipitation over China based on CMIP5 models. *Adv. Atmos. Sci.*, **32**, 487–496, https://doi.org/10.1007/s00376-014-4102-7.

Tian, F. X., B. W. Dong, J. Robson, R. Sutton, and S. F. B. Tett, 2019: Projected near term changes in the East Asian summer monsoon and its uncertainty. *Environmental Research Letters*, **14**, 084038, https://doi.org/10.1088/1748-9326/ab28a6.

Trenberth, K. E., and C. J. Guillemot, 1995: Evaluation of the global atmospheric moisture budget as seen from analyses. *J. Climate*, **8**, 2255–2272, https://doi.org/10.1175/1520-0442(1995)008<2255:EOTGAM>2.0.CO;2.

Vannière, B., and Coauthors, 2019: Multi-model evaluation of the sensitivity of the global energy budget and hydrological cycle to resolution. *Climate Dyn.*, **52**, 6817–6846, https://doi.org/10.1007/s00382-018-4547-y.

Wang, Y. J., B. T. Zhou, D. H. Qin, J. Wu, R. Gao, and L. C. Song, 2017: Changes in mean and extreme temperature and precipitation over the arid region of northwestern China: Observation and projection. *Adv. Atmos. Sci.*, **34**, 289–305, https://doi.org/10.1007/s00376-016-6160-5.

Wei, K., T. Xu, Z. C. Du, H. N. Gong, and B. H. Xie, 2014: How well do the current state-of-the-art CMIP5 models characterise the climatology of the East Asian winter monsoon? *Climate Dyn.*, **43**, 1241–1255, https://doi.org/10.1007/s00382-013-1929-z.

Wu, J., and X. J. Gao, 2013: A gridded daily observation dataset over China region and comparison with the other datasets. *Chinese Journal of Geophysics*, **56**, 1102–1111, https://doi.org/10.6038/cjg20130406. (in Chinese with English abstract)

Xin, X. G., T. W. Wu, J. Zhang, J. C. Yao, and Y. J. Fang, 2020: Comparison of CMIP6 and CMIP5 simulations of precipitation in China and the East Asian summer monsoon. *International Journal of Climatology*, **40**, 6423–6440, https://doi.org/10.1002/joc.6590.

Xu, Y., and C. H. Xu, 2012: Preliminary assessment of simulations of climate changes over China by CMIP5 multi-models. *Atmospheric and Oceanic Science Letters*, **5**, 489–494, https://doi.org/10.1080/16742834.2012.11447041.

Yang, X. L., B. T. Zhou, Y. Xu, and Z. Y. Han, 2021: CMIP6 evaluation and projection of temperature and precipitation over China. *Adv. Atmos. Sci.*, **38**, 817–830, https://doi.org/10.1007/s00376-021-0351-4.

Yao, J. C., T. J. Zhou, Z. Guo, X. L. Chen, L. W. Zou, and Y. Sun, 2017: Improved performance of high-resolution atmospheric models in simulating the East Asian summer monsoon rain belt. *J. Climate*, **30**, 8825–8840, https://doi.org/10.1175/JCLI-D-16-0372.1.

Yuan, W. H., 2013: Diurnal cycles of precipitation over subtropical China in IPCC AR5 AMIP simulations. *Adv. Atmos. Sci.*, **30**, 1679–1694, https://doi.org/10.1007/s00376-013-2250-9.

Zhang, D. P., Y. Y. Huang, B. T. Zhou, and H. J. Wang, 2021: Is there interdecadal variation in the South Asian High. *J. Climate*, **34**, 8089–8103, https://doi.org/10.1175/JCLI-D-21-0059.1.

Zhou, B. T., Y. Xu, and Y. Shig, 2018a: Present and future connection of Asian-Pacific Oscillation to large-scale atmospheric circulations and East Asian rainfall: Results of CMIP5. *Climate Dyn.*, **50**, 17–29, https://doi.org/10.1007/s00382-017-3579-z.

Zhou, B. T., Q. H. Wen, Y. Xu, L. C. Song, and X. B. Zhang, 2014: Projected changes in temperature and precipitation extremes in China by the CMIP5 multimodel ensembles. *J. Climate*, **27**, 6591–6611, https://doi.org/10.1175/JCLI-D-13-00761.1.

Zhou, S. J., G. Huang, and P. Huang, 2020: Inter-model spread of the changes in the East Asian summer monsoon system in CMIP5/6 Models. *J. Geophys. Res.: Atmos.*, **125**, 2020JD033016, https://doi.org/10.1029/2020JD033016.

Zhou, T. J., and Z. X. Li, 2002: Simulation of the East Asian Summer Monsoon using a variable resolution atmospheric GCM. *Climate Dyn.*, **19**, 167–180, https://doi.org/10.1007/s00382-001-0214-8.

Zhou, T. J., and Coauthors, 2018b: A review of East Asian summer monsoon simulation and projection: Achievements and problems, opportunities and challenges. *Chinese Journal of Atmospheric Science*, **42**, 902–934, https://doi.org/10.3878/j.issn.1006-9895.1802.17306. (in Chinese with English abstract)

Zhu, H. H., Z. H. Jiang, J. Li, W. Li, C. X. Sun, and L. Li, 2020: Does CMIP6 inspire more confidence in simulating climate extremes over China? *Adv. Atmos. Sci.*, **37**, 1119–1132, https://doi.org/10.1007/s00376-020-9289-1.